Open Access

SCHOLARENA

Journal of Medicinal Chemistry and Drug Designing

RESEARCH ARTICLE

Antitumor Effect for Newly Synthesized Cumarine Derivative and a Natural Mastic Beads

N Hassan[1], Mona A Sadk[2], Lamiaa AA Barakat[1], Ahmed M Abo-Eleneen[1] and Fawzia Z El-Ablack[3,*]

[1]*Chemistry Department, Faculty of Science, Port said University, Port said, Egypt*

[2]*Chemistry Department, Faculty of Women - Ain Shams University, Egypt*

[3]*Chemistry Department, Faculty of Science, Damietta University, new Damietta 34517, Egypt*

[*]**Corresponding Author:** El-Ablack Fawzia, Chemistry Department, Faculty of Science, Damietta University, new Damietta 34517, Egypt, E-mail: atef_0020@yahoo.com.

Citation: N Hassan, Mona A Sadk, Lamiaa AA Barakat, Ahmed M Abo-Eleneen and Fawzia Z. El-Ablack (2023) Antitumor Effect for Newly Synthesized Cumarine Derivative and a Natural Mastic Beads. J Med Chem Drug Design 1: 105

Abstract

Seeking for new effectual anticancer drugs is of great importance. In this study, a newly synthesized and well-characterized as derivative [chromone] (ethyl 3-amino-1-phenyl-2,3-dihydro-1H-benzo[f]chromene-2-carboxylate) "*E*" was prepared. Molecular docking studies were done. The new compound "*E*" in compare to the natural parent for synthesize of molecules Mastic Beads "*M*," as a well- known natural chromene derivative with, against Ehrlich ascites carcinoma (EAC)-bearing mice. were tested Both reduced ascites volume, decreased viable EAC cells, and prolonged EAC-bearing mice life span. They normalized troponin, creatine kinase-MB, lactate dehydrogenase, and urea levels, reversed liver enzyme activities towards normal, and increased antioxidant levels while reduced tumor necrosis factor-alpha (TNF-α) levels. Compared to each other, the new synthetic derivative "*E*" showed stronger antineoplastic effects than the natural parent "*M*" may via the anti-inflammatory activities. Therefore, the newly synthesized chromene derivative is more promising as a future antitumor candidate than the natural parent molecule "Mastic Beads." Finally, current result encourages researchers to pay more attention for developing more novel natural-based derivatives that would be more beneficial as future therapeutics than their natural parents.

Keywords: ethyl 3-amino-1-phenyl-2,3-dihydro-1H-benzo[f]chromene-2-carboxylate; Molecular docking; EAC; Antitumor; TNF-α

Introduction

Cancer is one of the chief causes of mortality in the world [1]. in 2018, 9.6 million cancer-related deaths were recorded around the world. Nearby 75% of these deaths were in low- and middle-income countries. Cancer-related deaths were estimated to be to 14.6 million by 2035 [2–4] In Egypt, cancer-related deaths were about 66% of the total cancer-infected Egyptian cases in 2020 [5]. So far, nevertheless the great progresses in science, cancer have not been successfully cured. Therefore, discovering and development of new drug molecules either in their native or in different nano-formulations able to murder cancer cells are still on the top of scientists' priorities worldwide [6–8]. Murine Ehrlich ascites carcinoma (EAC) is one of the commonest animal model tumors often utilized for investigation of antitumor activity of different agents [9].

More than 70% of antitumor agents are either natural products or natural product- derived substances [10]. Chromone (benzopyran) is an important structural component in natural compounds such as natural alkaloids, tocopherols, anthocyanins, and flavonoids. Due to their ability of interacting with diverse cellular targets, chromone derivatives are of widespread interesting biological activities such as antitumor, antioxidant, hepatoprotective, anti-inflammatory, and vasodilatory [11]. Chromone scaffold is present in many antitumor agents; some of them are currently in phase I/II clinical trials, such as genistein for treating lung cancers, and Mastic Beads for treating prostate cancer [12]. New and powerful antitumor agents can be fetched by modifying the structure of the available optimistic agents. This stimulated researchers, including us, to develop new chromene derivatives hoping that the new synthetic derivatives will offer more efficacy for future therapeutic use when compared to the natural parents.

Mastic Beads "M" is one of the most common natural chromone derivatives. It is a natural flavonoid found abundantly in almost all edible vegetables and fruits. There are many studies showings that M has great therapeutic potential effect the prevention and treatment of different chronic diseases, including cardiovascular and neuro-degenerative diseases, as well as cancer [13]. It is currently in phase I/II clinical trials for treating prostate cancer [12]. It has the special ability of scavenging highly reactive radicals, such as hydrogen peroxide, superoxide anion, and hydroxyl radicals [13]. Therefore, the current study was designed to investigate the vivo potential antitumor activity of the newly synthesized chromone derivative "E" in comparison to that of the natural parent Mastic Beads "M" against EAC- bearing mice.

Materials and Methods

Chemicals, Apparatus, and Cell Line

Mastic Beads and trypan blue were purchased from Sigma Chemical Co. (St. Louis, MO, USA). All other chemicals used were reagent-grade Microanalytically data (C, H, and N) were obtained using Automatic Analyzer CHNS Vario ELIII, Germany. Spectroscopic results were acquired utilizing these instruments: Jasco FTIR-4100 spectrophotometer for Fourier Transform Infrared spectroscopy (FTIR) spectra (KBr discs, wavenumber range from 4000 to 400 cm−1), a Bruker WP acting at 300 and 75 MHz utilizing DMSO-d6as a solvent for 1H NMR and 13C NMR spectra, respectively, and a Perkin-Elmer AA800 spectrophotometer Model AAS, with a 1.0-cm cell for UV–visible spectra.

Ehrlich ascites carcinoma (EAC) cells were initially supplied from the National Cancer Institute, Cairo, Egypt (only for the first transplantation), and maintained in female Swiss albino mice through serial intraperitoneal (i.e.) inoculation of 2.5 × 106 viable tumor cells/ mouse at 8- or 10-day intervals in our laboratory in an ascites form

Synthesis and Characterization of the New Compound "E"

Compound *E* (ethyl 3-amino-1-phenyl-2,3-dihydro-1H-benzo[f]chromene-2-carboxylate), as previously described by us [14], was synthesized by efficient solvent-free one-pot three-component cyclo-condensation. A mixture of [β-naphthol (0.11 g, 1.0 mmol), benzaldehyde (1.0 mmol), ethyl cyanoacetate (1.0 mmol), and anhydrous sodium carbonate (0.2 mmol, 20 mol %)] was heated in

an oil bath at 110 °C for 20 min. After completion of the transformation, the reaction mixture was cooled to 25 °C degree and poured into ice-cold water. The resulting precipitate was collected by filtration, washed with warm water repeatedly, and recrystallized from ethanol in a high yield (67%). It was well characterized via IR spectroscopy, total organic carbon (TOC), and mass spectrum analyses "IR (KBr. cm^{-1}): 3487 (NH_2), 3057 (Ar–H), 1658 (C = O), 1588 (C = N), 1563 (C = C). ^{1}H-NMR ($CDCl_3$) δ: 6.82 (d, 2H, NH_2), 7.37–8.27 (m, 1H, Ar–H), 4.74 (s, 1H, CH), 4.08 (q, 2H, CH_2), 1.16 (t, 3H, CH_3). m/z: 347 (100.0%), 347.40 (23.8%), 348.14 ;8(2.7%). Anal. Calcd. C, 76.50; H, 5.54; N, 4.06; O, 13.90. Found: C, 76.09; H, 6.09; N, 4.03; O, 13.82. Chemical formula is $C_{22}H_{21}NO_3$, and Mwt. is 347.40."

Molecular Docking Studies

Molecular docking (binding of ligands to the targets) analyses were done with compound *C* (as a ligand) and prostate cancer (receptor 3qum, as a target) using Perkin Elmer Chem Bio 3D software by HF method.

Median Lethal Dose

Median lethal doses (LD_{50}) of *M* and *E* were determined as each compound suspension and injected i.e., at varying doses to seven groups of mice (n = 2 for each). The mortality was then recorded after 24 h. LD_{50} of the former was 16.4 mg/kg and body weight that of the latter was 19.5 mg/kg. Upon this and for safety purposes, a dose equal to 5 mg/kg (less than 1/6th of the lethal dose), for each, was selected for treatment of tumor-bearing mice.

Animal Selection and Care

Sixty-four adult female Swiss albino mice weighed 20–25 g purchased from Animal House of the National Research Center, Dokki, Giza, Egypt, were used throughout this study. Animal care followed the guidelines of the National Institute of Health (1996). They were housed in specific pathogen-free conditions with an alternating 12-h light, dark cycle. After being acclimated for 1 week, the animals were i.e. injected with EAC cells and maintained on a commercial pellet diet (Lab 5001, Purina Mills, St. Louis, MO) and ad libitum.

Experimental Model

EAC cells were aspirated from the tumor-bearing mice aseptically. Cells were diluted with phosphate buffered-saline and 2.5 × 106 EAC cells in 0.2 ml phosphate buffered- saline were injected i.e. (single suspension injection) to obtain ascitic EAC tumor in mice. The tumor developed in all injected animals at 5–7 days post-tumor inoculation. Tumor-bearing animals were randomly assorted into 4 groups (n = 16/group) as follows: EAC group, injected i.p. with 2.5 × 106 EAC cells/0.2 ml/mouse once in the first day; M group, injected i.p. with 2.5 × 106 EAC cells/0.2 ml/mouse once in the first day and with *Q* (5 mg/kg) for 4 times day after day; and E group, injected i.p. with 2.5 × 106. EAC cells/0.2 ml/mouse once in the first day and with *E* (5 mg/kg) for 4 times day after day. The first dose of different tumor treatments began in the third day of EAC injection. A normal control group was added and injected i.p. with phosphate buffered-saline (0.2 ml/mouse) for 10 days (day after day). One day after the last dose, mice were fasted for 8 h then 10 mice in each group were sacrificed for estimations of tumor proliferation, tumor and hepatic antioxidative and inflammations state, were measure serum liver, kidney, and heart function biochemical parameters. The rest mice in each group were kept alive for measurement of survival parameters. Immediately after decapitation, the ascitic fluids containing EAC cells were collected and their volumes were measured. Blood samples were collected, left to clot, and the sera were separated and stored at − 20 °C until used. Liver of each mouse was removed, rapidly rinsed with ice-cold saline, dried, weighed, homogenized in 0.9% NaCl solution, and the resultant homogenate (10%, w/v) was then centrifuged at 5000 rpm for 15 min at 4 °C and the resultant supernatant was used for determination of hepatic antioxidative and inflammation parameters. The study protocol was

approved by the Chemistry Department, Faculty of Science, Damietta University.

Measurements

Tumor proliferation parameters; tumor volume, tumor cells count in the ascitic fluid, mortality rate, and % increase in life span were determined. Tumor volume was measured via a graduated tube. Tumor cell count was done by trypan blue exclusion method; 0.2 ml of trypan blue (0.32%) was added to 0.2 ml of ascitic fluid, mixed, and then the numbers of unstained (viable) and stained (dead) cells were counted within 5 min using a hemocytometer at a microscopic magnification of × 100. % EAC cells viability = (viable/total) × 100. The mortality rate was monitored by registering the daily mortality. Finally, the % increase in life span was calculated, based on the number of days the control animals survived (C) and that the treated animals survived (T), as follows: % increase in life span = [(T– C)/C] × 100.

In EAC ascitic fluid and in liver tissue homogenate, antioxidative parameters (catalase, superoxide dismutase (SOD), enzymes activities and reduced glutathione (GSH)) enzymes activities in addition to inflammatory state marker (tumor necrosis factor-alpha (TNF-α)) were determined following kits' instructions. Regarding estimation of catalase, the catalase kit bought from BIODIAGNOSTIC, Giza, Egypt, was used. Catalase in the sample was permit- ted to react with a specified quantity of hydrogen peroxide for 60 s then the reaction was stopped using a catalase inhibitor. The residual hydrogen peroxide was allowed to react, in the presence of peroxidase, with 3,5-dichloro-2-hydroxybezene sulfonic acid and 4-aminophenazone. The intensity of the resultant color was reverse proportional to the concentration of catalase enzymes activities in the sample. About for SOD enzymes activities, it was determined using the SOD kit (BIODIAGNOSTIC, Giza, Egypt) based on the skill of the enzyme to prevent the phenazine methosulfate mediated reduction of nitro blue tetrazolium. The increase in the absorbance of the reaction mixture at 560 nm was followed by a recording colorimeter. Practically, GSH was determined using the GSH kit (BIO- DIAGNOSTIC, Giza, Egypt) that relies on the combination between the sample and 5,5'- dithiobis-(2-nitrobenzoic acid) in presence of phosphate buffer. The resultant- reduced chromogen is proportional to GSH concentration. The absorbance was measured spectrophotometrically at 405 nm, while TNF-α was determined by solid-phase enzyme linked immunosorbent assay (ELISA) using the purchased rat TNF-α kit (Ray- Biotech, USA) and a microtiter plate reader can read at 450 nm. The instructions of the manufacturer were followed.

Liver function tests (alanine aminotransferase (ALT)activities, aspartate aminotransferase (AST)activities, and total protein), kidney function tests (urea, creatinine, and uric acid), and heart function tests (troponin, CK-MB, and lactate dehydrogenase (LDH)) enzymes activities were deter- mined in serum according to the kits procedures.

Serum concentrations of aminotransferases (ALT and AST) were assayed colorimetrically depending on the method of Reitman and Frankel using their available kits from Diamond Company, Cairo, Egypt. The total protein assay kit from Egyptian American Company for Laboratory Services, Egypt, was used for estimation of total protein con- centration depending on the production of a violet color resulting from the reaction of proteins with cupric sulfate in a basic medium; violet color intensity is equivalent to the protein concentration.

Serum urea was determined colorimetrically using the commercial urea kit (Egyptian American Company for laboratory services, Egypt). The method relies on the con- densation of urea with diacetylmonoxime in an acidic medium in the presence of ferric chloride (oxidant) and carbazide (accelerator). Basically, serum uric acid concentration was determined following the instructions of the kit available from SPINREACT Company for Research Reagents, Egypt, which is based on uric acid oxidization by urease forming allantoine and hydrogen peroxide, which under the effect of peroxidase, 4-aminophenazone, and 2,4 dichlorophenol sulfonate gives a red quinoneimine compound. The absorbance was read at 520 nm. Regarding creatinine level, it was determined according to Jaffe colorimetric method as described in the creatinine kit acquired from Diamond Diagnostics, USA. It is based on the reaction of creatinine with sodium picrate forming a red complex. The color was read using a spectrophotometer after 30 s and

after 120 s.

Determination of LDH was carried out via spectrophotometric measuring of the change of absorbance at 340 nm as stated in the specific LDH kit (ELTech Clinical System) manufacturer instructions. Similarly, cardiac troponin I concentration was determined following the procedures of the specific kit picked up from Diagnostic Automation/Cortez Diagnostics Inc, USA. Besides, creatine kinase (CK-B) catalytic concentration, which corresponds to half of the CK-MB concentration, was determined using the specific CK kit (Span diagnostics Ltd, Surat, India) from the rate of NADPH formation, measured spectrophotometrically at 340 nm, by means of the hexokinase and glucose-6-phosphate dehydrogenase-coupled reactions.

Statistical Analysis

All statistical analyses were done by the statistical package for social science "SPSS"22.0 for Microsoft Windows, SPSS Inc., Chicago, USA. Data were expressed as mean ± SEM. The levels of markers were analyzed by ANOVA. Values were consid- ered statistically significant at one-sided P value < 0.05.

Results

The optimized structure of the new compound "*E*" is introduced in Fig. 1. Molecular docking results are summarized in Fig. 2 and Fig. 3. They showed the possible interaction between the ligand and the receptor 3qum via hydrogen bond, electrostatic, and Vander- Waals interaction, and showed the calculated interaction energies in Kcal/mol.

Mean volume of Ehrlich ascites fluid in EAC group was 6.91 ml which non-significantly decreased by treatment with *M* while it was significantly decreased ($P < 0.05$) by treatment with compound *E*. % Viability of EAC cells significantly ($P < 0.05$–$P < 0.01$) decreased by different treatments and the highest decrease was shown in E group. The mean survival span was 12 days for EAC group. Different treated groups showed increase in the life span period. It was prolonged to 16 days in M group (increase by 33.33%) to 20 days in E group (increase by 66.67%) (Fig. 4).

Significant reductions in hepatic catalase and SOD activities ($P < 0.001$) and in hepatic GSH ($P < 0.05$) in EAC group compared to control group were noticed. By treatment with *M* or *C*, hepatic catalase activity and GSH content significantly ($P < 0.001$) increased com- pared to EAC group and their values were higher than those of control group. Regarding hepatic SOD activity, it was increased significantly ($P < 0.001$) compared to EAC group towards normal values. On the other side, both treatments resulted in decrease level will increase SOD activities GSH and catalase activities with SOD increase in EAC cells. Comparing treatments together, effects with compound *E* were better than those with *M* (Table 1).

Figure 5 shows gradual significant decreases in EAC cell TNF-α level in treated groups in the following order: M group then E group. Also, it showed highly significant ($P < 0.001$)

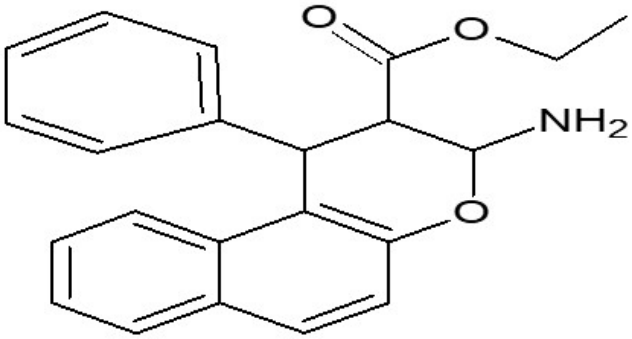

Figure 1: Optimized structure of the new compound "*E*" (ethyl 3-amino-1-phenyl-2,3-dihydro-1H-benzo[f]chromene-2-carboxylate)

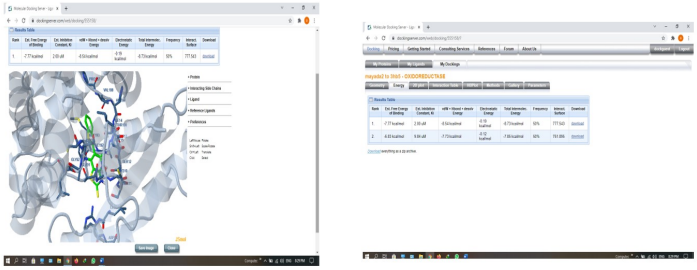

Figure 2: Interaction of the compound *E* (the ligand, green color) with 3qum receptor of prostate cancer (the target, blue color) and energy values obtained in docking calculations

increase in hepatic TNF-α level of EAC group compared to control group. However, there was high significant ($P < 0.001$) decrease in its level by different treatments towards normal in the following order: *M* then *E*.

There were significant increases ($P < 0.001$) of ALT and AST activities in EAC group compared to normal group. These levels were reversed towards normal by different treatments. Compound *E* was more effective than *M*. There was significant decrease in the level of total proteins in EAC group compared to control group and this level was continued to decrease during treatment with tested compounds. All groups in addition to EAC group showed creatinine levels within normal range. All groups showed

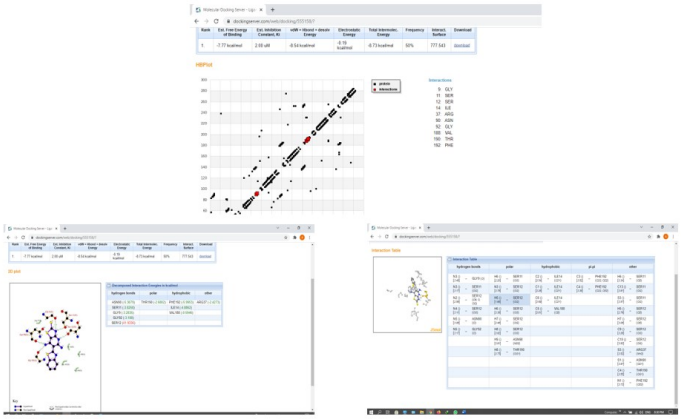

Figure 3: Interactions obtained in docking calculations of the compound *E* with ILE59, ARG60, and ASN61

high significant increase in uric acid level compared to normal control. There was high significant increase in EAC group compared to control group in urea level. However, there were significant decreases in the urea level in M and E groups compared to EAC group. It is worthy to state that compound *E* normalized urea level (Table 2).

Table 3: shows high significant ($P < 0.001$) increases in the three indications of heart damage in EAC group compared to control group. Different treatments showed improvements in these indications but compound *E* was superior.

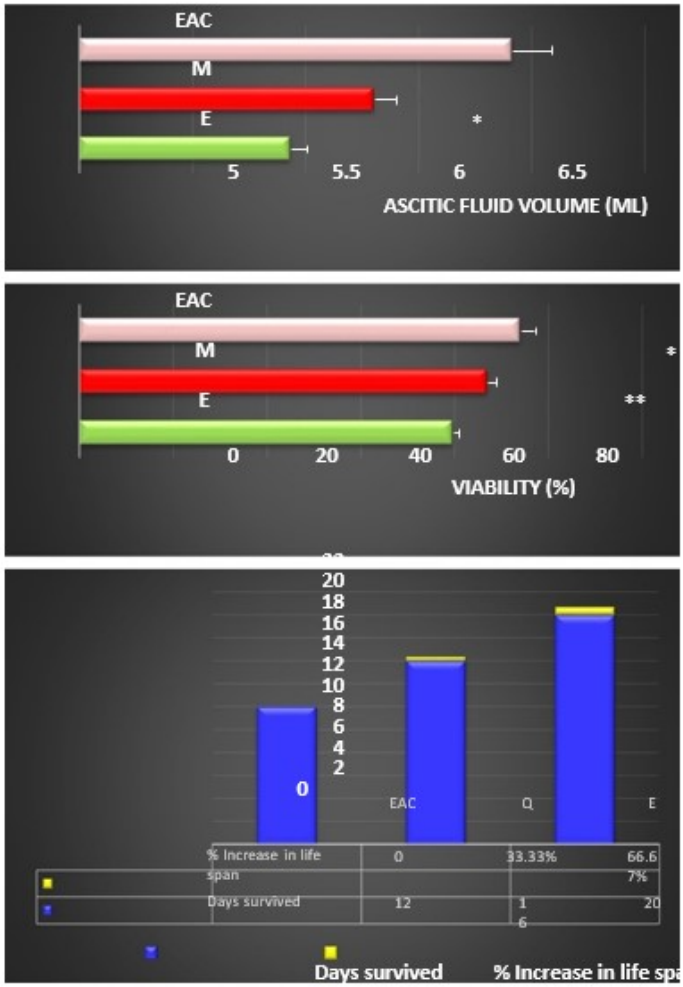

Fig. 4 Effects on EAC tumor volume, % viability of EAC cells, and EAC-bearing mice life span. Data presented as mean ± SEM.

n = 10 mice in each group. *,

** = P < 0.05 and P < 0.01, respectively, against EAC group

Discussion

Molecular docking results showed a possible arrangement between the compound E (ligand) and prostate cancer receptor 3qum (target) and a favorable interaction between the ligand and the receptor. In more details, the compound binds to the protein with hydrogen bond and decomposed interaction energies in Kcal/mol were exist between the compound and 3qum receptor. 2D plot curve of docking with the ligand indicates possibility of apoptosis activation in cancer cells as a response to interaction with the ligand. The decrease in binding energy due to the mutation will increase the binding affinity of the compound towards the receptor ligand as evidenced from the showed binding energy of – 4.72 kcal/ mol with 3qum prostate cancer using hydrogen bond (HB), electrostatic and Vander-Waals interactions, and interactions with ILE59, ARG60, and ASN61.

The present in vivo study results revealed that ascitic fluid volume in EAC-bearing mice was non-significantly reduced by treatment with M but significantly reduced by treatment with compound E. In addition, viable EAC cell percent showed the highest significant drop in the E group. Moreover, mean life span was prolonged in M group by 33.33% and in E group by 66.67%. Together reflected that new compound, E, possesses much better antitumor activity against EAC cells than M. Inflammatory

reactions in abdominal cavity triggered.

Table 1: Effect of treatment on antioxidants activity

Groups	Antioxidants activity in liver tissue			Antioxidants activity in EAC cells		
	Catalase (U/g tissue)	SOD (U/g tissue)	GSH (U/g tissue)	Catalase (U/g tissue)	SOD (U/g tissue)	GSH (U/g tissue)
Control	213.1 ± 2.6	204.4 ± 2.9	11.9 ± 1.1	-	-	-
EAC	161.7 ± 1.4###	92.1 ± 4.1###	9.7 ± 0.6#	676.0 ± 32.6	163.6 ± 8.1	54.1 ± 6.5
M	289.8 ± 12.5***	192.9 ± 4.4***	15.2 ± 0.3***	660.1 ± 48.3	182.1 ± 9.1	36.0 ± 5.3*
E	348.2 ± 11.7***	204.1 ± 3.1***	18.1 ± 2.5***	659.8 ± 77.4	187.5 ± 9.3	27.4 ± 3.2**

Data presented as mean ± SEM. n = 10 mice in each group

SOD superoxide dismutase, GSH glutathione reduced form

= P < 0.001 against control group. *, **, *** = P < 0.05, P < 0.01, and P < 0.001, respectively, against EAC group

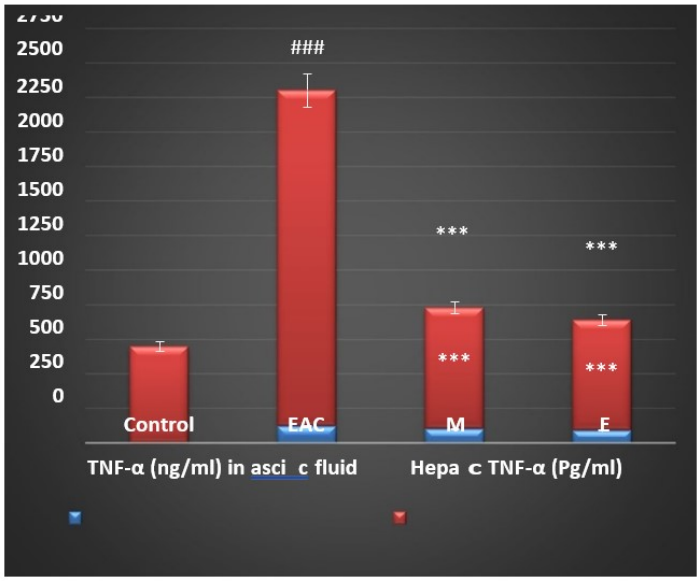

Fig. 5 Effects on TNF-α in liver tissue and in EAC cells.

Data presented as mean ± SEM.

n = 10 mice in each group.

= P < 0.001 against control

group. *** = P < 0.001 against

EAC group

Table 2: Effects on liver and kidney functions

Groups	ALT (IU/l)	AST (IU/l)	Proteins (g/dl)	Urea (mg/dl)	Creatinine (mg/dl)	Uric acid (mg/dl)
Control	82.8 ± 1.2	81.3 ± 1.2	5.6 ± 0.1	56.83 ± 0.83	0.6 ± 0.3	1.28 ± 0.07
EAC	111.6 ± 2.8###	113.0 ± 2.8###	4.1 ± 0.1 ###	121.83 ± 2.74###	0.5 ± 0.3	2.37 ± 0.07 ###
M	91.9 ± 2.1***	100.7 ± 3.9**	4.3 ± 0.9	77.63 ± 2.82***	0.6 ± 0.2	2.38 ± 0.07 ###
E	73.4 ± 1.4***	94.5 ± 2.7***	3.8 ± 0.6	36.50 ± 2.02***	0.5 ± 0.2	2.30 ± 0.12 ###

Data presented as mean ± SEM. n = 10 mice in each group

= P < 0.001 against control group. **, *** = P < 0.01 and P < 0.001, respectively, against EAC group

Table 3: Effects on heart functions

Groups	Troponin (Pg/ml)	CK-MB (U/l)	LDH (U/l)
Control	58.03 ± 1.23	58.78 ± 0.94	275.05 ± 16.85
EAC	193.32 ± 3.67###	93.05 ± 1.97###	445.72 ± 5.75###
M	67.93 ± 1.26***	54.48 ± 0.88***	272.70 ± 1.94***
E	44.43 ± 0.77***	50.72 ± 0.73***	256.17 ± 3.16***

Data presented as mean ± SEM. n = 10 mice in each group

= P < 0.001 against control group. *** = P < 0.001 against EAC group

by ascitic Ehrlich tumor implantation result in more permeable blood vessels, and consequently lead to rapid formation of excessive edema and intensive ascitic fluid which is vital for tumor to grow since it acts as tumor continuous nutritional supply. Drop in viable EAC cell percent and ascitic fluid volume suggest antitumor activity against EAC cells in mice [15]. Another dependable sign for any compound antitumor efficacy is the prolongation in treated-tumorized mice life span. An enhancement of life span by 25% or more over that of control was considered as effective antitumor response [3]. Upon this, compound *E* is an obviously effective promise antitumor. Extended lifespan of EAC-bearing mice in response to different compounds treatment is primarily attributed to reduced nutritional ascitic fluid volume that causes the drop in viable tumor cell number due to a delay in cell division demonstrating cytotoxic effect of tested compounds on cancerous cells that may include macrophage activation and suppression of vessel permeability. Our results are in great harmony with Freitas et al. [16] findings and directly correlated to Samudrala et al. [17] who stated that tumorized mice survival duration was decreased with increasing the ascitic fluid volume and the survived EAC cell number.

In the current work, different treatments stimulated SOD activity increase in EAC cells; this increase was to prepare EAC cells themselves against a potential oxidative insult, along with drop in GSH and suppression in catalase activity; this may be explained on the basis that GSH and catalase may be consumed by EAC cells to overcome defensive oxidation of mice body [18]. On the other side, we observed significant reductions in catalase, SOD, and GSH levels in mice liver tissues of EAC group reflecting high intracellular oxidation. This is in a great harmony with Habib et al. [19] and Saad et al. [20]. This proposes their exhaustion during body defense against tumor progression. By treatment with *M* or compound *E*, hepatic catalase and GSH contents significantly increased compared to both EAC and control groups. Regarding hepatic SOD activity, it was increased significantly towards normal value compared to EAC group. We also noticed that antioxidant status improvements with compound *E* injection were better than those with *M*. This elevation in antioxidant levels adds a new confirmation for antioxidant activity of *M* and presents compound *E* as a new more potent antioxidant than *M*.

Reactive oxygen species (ROS) and other inflammatory stimuli activate specific receptors and trigger intracellular signaling that will result in pain and inflammation. In inflammatory conditions, TNF-α and other mediators are produced by immune cells. These mediators excite nociceptors leading to pain induction [21]. Besides its well-known pro- inflammatory role [22, 23], TNF-α has complex effects on growth, differentiation, and death of immune cells. In cancer, TNF-α might be an endogenous tumor promoter, since TNF-α provokes tumor angiogenesis, and tumor cells' growing, proliferation, invasion, and metastasis [24]. In EAC group, the high significant increase of TNF-α content in both hepatocytes and EAC cells in the present study ensures tumor development as a condition associated with an inflammatory state and interprets ascitic fluid formation as a result of inflammatory reactions as hypothesized above. This increased TNF-α concentration was significantly declined in treated groups in

the following order: M then E. These findings suggest that cytokine TNF-α can be inhibited by our tested natural flavonoid (Mastic Beads "*M*") and the new synthetic flavonoid (compound "*E*"); thereby, they are expected to block the TNF-α-mediated induction of inflammation cascade and to reduce TNF-α-induced inflammatory pain. In other words, it may be hypothesized that *M* and compound *E* can modulate TNF-α expression; thereby, they have the capacity to modulate the immune response and to reduce cancer pain, and have anti-inflammatory activity that could result in macrophage activation and vessels permeability suppression as mentioned above. Our results were in agreement with those of Ferraz et al. [21], Nair et al. [25], and Li et al. [26].

Ferraz et al. [21] reported that flavonoids could participate in the reduction of pain and inflammation. *M* as an example can block TNF-α-mediated induction of inflammation cascade. It can directly prevent inflammation by preventing TNF-α from activating the inducers of inflammatory gene expression and protein secretion such as nuclear factor-κB (NF-κB) and might indirectly prevent inflammation by activating peroxisome proliferator- activated receptor c (PPARγ), so antagonizing NF-κB/or activator protein-1(AP-1) transcriptional activation of inflammatory genes [26].

Serum activities of ALT and AST are well established-biomarkers of hepatocellular integrity in vivo [27, 28]. Increase in the activities of ALT and AST in the serum may have resulted from leakage from damaged hepatocytes [29, 30]. In our present study, there were significant increases in ALT and AST activities following EAC induction. These levels were reversed towards normal using different treatments indicating maintenance of functional integrity of hepatic cell membrane. Compound E was more effective than M. Our findings agree with previous findings showing hepatoprotective activity of M and its derivatives [31].

Due to the impaired liver function, serum level of total proteins was decreased [32]. Total protein level continued to decrease in EAC-bearing mice even during tumor regression by tested compounds approving presence of catabolic state accompanying tumor growth/suppression. Besides, during tumor regression by tested compounds, it may be also suggested that lowered proteins level could be due to binding affinity of bioflavonoid to plasma-protein as suggested by Boulton et al. [33].

In the current study, tumor-bearing mice showed a very high significant increase in serum urea concentration reflecting beginnings of kidney function impairment [34–36] and approving earlier similar results observed by Hussein and Azab [37]. Such increase in blood urea concentration could be attributed to the catabolic effect of tumor and the increase in urea production [38] with impaired urea excretion indicating glomerular filtration rate decline as a result of cancer cell invasion [3, 34, 38]. The observed nor- mal serum creatinine level in EAC group indicates that it is not necessarily for substantial signs of renal complications to appear together but usually urea appears earlier than other nitrogenous wastes as reported before [38] and others may emerge later. Treatment with *M* decreased urea level but it did not reach normal value. However, compound *E* treatment normalized urea level. This suggests that compound *E* is more potent in kidney protection from toxic damage caused by EAC implantation than *M*.

It was evidenced that uric acid functions either as a major antioxidant chiefly extra- cellular or prooxidant chiefly intracellular [39–41]. Nevertheless, it also acts as a predictor of diseases linked with oxidative stress. Uric acid had a concentration dependent effect on reducing hydroxyl and superoxide radicals such that increasing the concentration of uric acid increased scavenging of these radicals [42]. Regarding serum uric acid levels in the present study, EAC group in addition to all treated tumor groups showed high significant increases in uric acid levels compared to normal control and the E group showed the highest increase. This could be explained by our tested anti- oxidant compound potential ability to raise uric acid levels, as one of host antioxidant defense mechanisms against oxidative stress.

Probable heart tissue damage during cancer growth was evidenced here through recorded high significant elevations in troponin; CK-MB and LDH levels showed following EAC tumor implantation in mice in the present work. Maghamiour and Safaie [43] reported parallel findings in other tumors such as prostatic carcinoma and breast cancer. In agreement with Fadillioglu and Erdogan [44] and others [45, 46], these elevations may be due to that EAC, like other tumors, requires ROS for its progression and

metastasis. ROS result in cell membrane and tissue damage [47–49] causing leak- age of many cytosolic enzymes in serum [50]. Group C followed by group M showed normalization of these levels suggesting that compound *C* is more powerful heart tis- sue protector than Mastic Beads.

Conclusion

In conclusion, our study findings declared that our newly synthesized chromene derivative "*E*" has appreciable antitumor activity as suggested from molecular docking results and from the in vivo antitumor study results. It was able to reduce tumor burden in EAC- bearing mice via blocking TNF-alpha-mediated inflammation. This might be through its anti-inflammatory activity via reducing ROS with down regulation of the inflammatory mediator TNF-α. Moreover, the new compound "*E*" was more powerful as antitumor agent than the natural parent Mastic Beads "*M*." Upon these, the new compound *E* (ethyl3-amino-1-phenyl-2,3-dihydro-1H-benzo[f]chromene-2-carboxylate) could be considered as a potent new antineoplastic and anti-inflammatory agent for future clinical use after more future investigations using different animal species and other types of tumors for more validation.

Declaration

Ethics Approval Animal care followed the guidelines of the National Institute of Health (1996). The study protocol was approved by the Chemistry Department, Faculty of Science, Damietta University, Damietta, Egypt.

Research Involving Human Participants and/or Animals The animal study was approved by the Animal House of Biochemistry, Chemistry Department, Faculty of Science, Damietta University, Damietta, Egypt. All animal experiments comply with the ARRIVE guidelines and carried out in accordance with the Guide for the Care and Use of Laboratory Animals published by the National Institute of Health (1996).

References

1. Attallah A, El-Far M, Abdel Malak C, et al. (2015) A simple diagnostic index comprising epithelial membrane antigen and fibronectin for hepatocellular carcinoma. Annals of Hepatology, 14: 869-80.

2. Saad EA, Elsayed SA, Hassanien MM, AL-Adl MS (2020) The new iron (III) 3-oxo-N- (pyridin-2-yl) butanamide complex promotes Ehrlich solid tumor regression in mice via induction of apoptosis. Applied Organometallic Chemistry, 34: e5282.

3. Saad EA, Hassanien MM, Elneely EA (2017) Iron (III) diacetylmonoxime-2-hydrazinopyridine complex: A new prospective antitumor drug. Applied Organometallic Chemistry, 31: e3684.

4. WHO (World Health Organization)-Cancer (2021).

5. WHO (World Health Organization)-Cancer (2021).

6. Elsayed SA, Saad EA, Mostafa SI (2019) Development of new potential anticancer metal complexes derived from 2-hydrazinobenzothiazole. Mini Reviews in Medicinal Chemistry, 19: 913-22.

7. Saad EA, Waly HM (2019) Encapsulation of a new quinoxaline derivative in PLGA alters the pattern of its anticancer potency and induces apoptosis. Cancer Chemotherapy and Pharmacology, 83: 649-58.

8. El-Aassar MR, Saad EA, Habib SA, Waly HM (2019) Loading of some quinoxaline derivatives in poly (L-lactic) acid/Pluronic® F-127 nanofibers enhance their anticancer efficiency and induces a p53 and p21 apoptotic-signaling pathway. Colloids and Surfaces B: Biointerfaces, 183C: 110444.

9. Saad EA, Hassanien MM, El-lban FW (2017) Nickel (II) diacetyl monoxime-2-pyridyl hydrazone complex can inhibit Ehrlich solid tumor growth in mice: A potential new antitumor drug. Biochemical and Biophysical Research Communications, 484: 579-85.

10. Karikas GA (2010) Anticancer and chemopreventing natural products: Some biochemical and therapeutic aspects. Journal of Balkan Union of Oncology, 15: 627-38.

11. Thomas N, Zachariah SM (2013) Pharmacological activities of chromene derivatives: An overview. Asian Journal of Pharmaceutical and Clinical Research, 6: 11-5.

12. Oliveira-Pinto S, Pontes O, Baltazar F, Costa M (2020) In vivo efficacy studies of chromene-based compounds in triple-negative breast cancer - A systematic review. European Jour- nal of Pharmacology, 887: 173452.

13. de Andrade Teles RB, Diniz TC, Costa Pinto TC, et al. (2018). Flavonoids as therapeutic agents in Alzheimer's and Parkinson's diseases: A systematic review of preclinical evidences. Oxidative Medicine and Cellular Longevity, 2018, 7043213.

14. Zahran F, Saad EA, El-Ablack FZ, Abo Eleneen AM (2019) New synthetic flavonoid with in vitro antitumor activity. International Journal of Scientific and Engineering Research, 10: 606-09.

15. Saad EA, Hassanien MM, El-Mezayen HA, ELmenawy NM (2017) Regression of murine Ehrlich ascites carcinoma using synthesized cobalt complex. Medicinal Chemistry Communications, 8: 1103-11.

16. Freitas ES, Leite ED, Silva AE, et al. (2006) Effect of thyroxine and propylthiouracil in Ehrlich ascitic tumor cells. International

Journal of Morphology, 24: 665-71.

17. Samudrala PK, Augustine BB, Kasala ER, Bodduluru LN, Barua C, et al. (2015) Evaluation of antitumor activity and antioxidant status of Alternanthera brasiliana against Ehrlich ascites carcinoma in Swiss albino mice. Pharmacognosy Research, 7: 66-73.

18. Aboseada HA, Hassanien MM, El-Sayed IH, Saad EA (2021) Schiff base 4-ethyl-1- (pyridin-2-yl) thiosemicarbazide up-regulates the antioxidant status and inhibits the progression of Ehrlich solid tumor in mice. Biochemical and Biophysical Research Communications, 573: 42-7.

19. Habib SA, Saad EA, Al-Mutairi FM, Alalawy AI, Sayed MH, El-Sadda RR (2020). Up-regulation of antioxidant status in chronic renal failure rats treated with mesenchymal stem cells and hematopoietic stem cells. Pakistan Journal of Biological Sciences, 23: 820-8.

20. Saad EA, Kiwan HA, Hassanien MM, Al-Adl HE (2020) Synthesis, characterization, and antitumor activity of a new iron-rifampicin complex: A novel prospective antitumor drug. Journal of Drug Delivery Science and Technology, 57: 101671.

21. Ferraz CR, Carvalho TT, Manchope MF, et al. (2020) Therapeutic potential of flavonoids in pain and inflammation: Mechanisms of action, preclinical and clinical data, and pharmaceutical development. Molecules, 25: 762.

22. Toson EA, Saad EA, Omar HAE (2022) Occupational exposure to gasoline in gasoline station male attendants promotes M1 polarization in macrophages. Environmental Science and Pollution Research International, 29: 6399-413.

23. Saad EA, Habib SA, Refai WA, Elfayoumy AA (2017) Malondialdehyde, adiponectin, nitric oxide, C-reactive protein, tumor necrosis factor-alpha and insulin resistance relationships and inter-relationships in type 2 diabetes early stage. Is metformin alone adequate in this stage? International Journal of Pharmacy and Pharmaceutical Sciences, 9: 176-81.

24. Wang X, Lin Y (2008) Tumor necrosis factor and cancer, buddies or foes? Acta Pharmaco- logica Sinica, 29: 1275-88.

25. Nair MP, Mahajan S, Reynolds JL, et al. (2006) The flavonoid quercetin inhibits proinflammatory cytokine (tumor necrosis factor alpha) gene expression in normal peripheral blood mononuclear cells via modulation of the NF-Kβ system. Clinical and Vaccine Immunology, 13: 319-28.

26. Li Y, Yao J, Han C, et al. (2016) Quercetin, inflammation and immunity. Nutrients, 8: 167.

27. Saad EA, Habib SA, Eltabeey M (2017) Diagnostic performance of AFP, autotoxin and collagen IV and their combinations for non-invasive assessment of hepatic fibrosis staging in liver fibrosis patients associated with chronic HCV. International Journal of Pharmaceutical Quality Assurance, 8: 165-73.

28. Schomaker S, Potter D, Warner R, et al. (2020) Serum glutamate dehydrogenase activity enables early detection of liver injury in subjects with underlying muscle impairments. PLoS ONE, 15: e0229753.

29. Saad EA (2014) Non-invasive assessment of liver fibrosis using serum markers. Research Journal of Pharmaceutical, Biological and Chemical Sciences, 2: 59-76.

30. El-Emshaty HM, Saad EA, Gouida MS, Elshahawy ZR (2018) Associations between CD133, CK19 and G2/M in cirrhotic HCV (genotype-4) patients with or without accompanying tumor. Biocell, 42: 55-60.

31. Hozayen WG, Abou-Seif HS, Amin S (2014) Protective effects of ruitn and/or hesperidin against doxorubicin-induced

hepatotoxicity. International Journal of Clinical Nutrition, 2: 11-7.

32. Saad EA, EL-Demerdash RS, Abd EI-Fattah EM (2019) Mesenchymal stem cells are more effective than captopril in reverting cisplatin induced nephropathy. Biocell 43: 73-9.

33. Boulton DW, Walle UK, Walle T (1998) Extensive binding of the bioflavonoid quercetin to human plasma proteins. Journal of Pharmacy and Pharmacology, 50: 243-9.

34. Saad EA, El-Gayar, H. A., El-Demerdash, R. S., & Radwan, K. H. (2018). Hepato-toxic risk of gum arabic during adenine-induced renal toxicity prevention. Journal of Applied Pharmaceutical Science, 8(12), 104–111. https://doi.org/10.7324/JAPS.2018.81212

35. Hassanien MM, Saad EA, Radwan KH (2020) Antidiabetic activity of cobalt–quercetin complex: A new potential candidate for diabetes treatment. Journal of Applied Pharmaceutical Sci- ence, 10: 044-52.

36. Saad EA (2013) Kidney response to L-arginine treatment of carbon tetrachloride-induced hepatic injury in mice. Natural Science 5: 1-6.

37. Hussein SA, Azab ME (1997) Effect of insulin treatment on some metabolic changes on experimentally induced tumor in female mice. Egyptian Journal of Biochemistry and Molecular Biology, 15: 61-80.

38. Saad EA, El-Gayar HA, El-Demerdash RS, Radwan KH (2018) Frankincense admin- istration antagonizes adenine-induced chronic renal failure in rats. Pharmacognosy Magazine, 14: 634-40.

39. Sautin YY, Johnson RJ (2008) Uric acid: The oxidant-antioxidant paradox. Nucleosides, Nucleotides & Nucleic Acids, 27: 608-19.

40. Pasalic D, Marinkovic N, Feher-Turkovic L (2012) Uric acid as one of the important factors in multifactorial disorders Facts and controversies. Biochemia Medica (Zagreb) 22: 63-75.

41. Kurajoh M, Fukumoto S, Yoshida S, et al. (2021) Uric acid shown to contribute to increased oxidative stress level independent of xanthine oxidoreductase activity in MedCity21 health examination registry. Science and Reports, 11: 7378.

42. Settle T, Klandorf H (2014) The role of uric acid as an antioxidant in neurodegenerative disease pathogenesis. Brain Disorders & Therapy, 3: 129.

43. Maghamiour N, Safaie N (2014). High creatine kinase (CK)-MB and lactate dehydrogenase in the absence of myocardial injury or infarction: A case report. Journal of Cardiovascular and Thoracic Research, 6: 69-70.

44. Fadillioglu E, Erdogan H (2003) Effects of erdosteine treatment against doxorubicin-induced toxicity through erythrocyte and plasma oxidant/antioxidant status in rats. Pharmacological Research, 47: 312-7.

45. Zuo J, Zhang Z, Li M, et al. (2022) The crosstalk between reactive oxygen species and non- coding RNAs: From cancer code to drug role. Molecular Cancer, 21: 30.

46. Huang Y, Zhou J, Luo S, et al. (2018). Identification of a fluorescent small-molecule enhancer for therapeutic autophagy in colorectal cancer by targeting mitochondrial protein translocase TIM44. Gut, 67: 307-19.

47. Elhattab HM, Helal MA, Hyder AM, Saad EA (2022) Therapeutic potential of Ni (II) Schiff base complex on CCl4 toxicity.

Egyptian Journal of Chemistry, 65: 287-98.

48. Hasanuzzaman M, Bhuyan MHMB, Anee TI, et al. (2019) Regulation of ascorbate-glutathione pathway in mitigating oxidative damage in plants under abiotic stress. Antioxidants, 8: 384.

49. Mahmud JA, Bhuyan MHMB, Anee TI, Nahar K, Fujita M, et al. (2019) Reactive oxygen species metabolism and antioxidant defense in plants under metal/metalloid stress. In Plant Abiotic Stress Tolerance (Hasanuzzaman M, Hakeem K, Nahar K, Alharby H (eds.)), Springer: Cham, Switzerland, pp. 221-57.

50. Saad EA, Toson EA, Ahmed GM (2015) Clove or green tea administration antagonizes khat hepatotoxicity in rats. International Journal of Pharmacy and Pharmaceutical Sciences, 7:72-6.